Available online at www.sciencedirect.com
ScienceDirect
Journal of the European Ceramic Society 28 (2008) 205–215
www.elsevier.com/locate/jeurceramsoc

Sintering behaviour and microstructural evolution of ultrapure α-alumina containing low amounts of SiO_2

Nicolas Louet, Helen Reveron *, Gilbert Fantozzi

Université de Lyon, INSA-Lyon, MATEIS CNRS UMR 5510, 20 Av. Albert Einstein, F-69621 Villeurbanne Cedex, France

Received 24 January 2007; received in revised form 22 March 2007; accepted 13 April 2007
Available online 13 August 2007

Abstract

The effect of small additions of silica (SiO_2) on the densification and microstructural evolution of an ultrapure α-alumina (Al_2O_3) has been investigated. The role of SiO_2 on the sintering behaviour was elucidated through an extensive dilatometric study performed on pure alumina and on doped samples with small amounts of colloidal silica (up to 2000 ppm). It has been found that the addition of SiO_2 leads to a significant decrease of the shrinkage rate at the intermediate state of sintering due to the reduction of point defects (predominantly oxygen vacancies). Doping with small amounts of SiO_2 results in heterogeneous microstructures in which abnormal grain growth was observed above a critical temperature of near 1600 °C. Below this temperature, silicon was detected at the grain-boundary triple junctions forming amorphous pockets and over 10 nm at each side of the grain boundaries. Above 1600 °C, a glassy phase of 2–3 nm in thickness was formed at the grain boundaries.

Keywords: Sintering; Microstructure-final; Al_2O_3; SiO_2

1. Introduction

Alpha-alumina (α-Al_2O_3) is one of the more widely used advanced ceramic materials because of its unique mechanical, electrical and optical properties. Since the properties exhibited by a ceramic are governed by its microstructure, refining α-alumina processing techniques to obtain superior microstructures is of great interest. Many macroscopic properties appear to be controlled by not only the microstructure but the chemistry of grain boundaries and interfaces. Grain boundaries in ceramics generally act as a sink for insoluble impurities or processing additives which often develop liquid phases during sintering forming thin amorphous films after cooling.

In recent years, numerous studies have been focused on the effect of small amount of additives, dopants or impurities on the sintering behaviour of ultrapure alumina. Such works have allowed a better comprehension of the densification process and microstructural evolution in commercial alumina powders which typically contain several thousands parts per million (ppm) of impurities such as magnesium, calcium and silicon[1–6] or trace amounts (<1000 ppm) of zirconium or rare-earth dopants such as yttrium, lanthanum and neodymium.[7–10] The use of magnesia has been very effective in controlling abnormal grain growth through a solid solution pinning mechanism and thus, achieving theoretical densities in MgO-doped alumina ceramics. Dopants forming liquid silicates (e.g. in the alumina–calcia–silica system) have achieved considerable importance because they provide many eutectics which can generate wetting liquid phases at the temperatures of 1200–1400 °C, allowing an excellent densification of alumina. However, the effect of each dopant oxide or impurity is still controversial because the initial impurities content of the raw materials, the processing methods or the sintering conditions vary between all the works done. It has been shown that the addition of small amounts of rare-earth dopants to fine-grained alumina (1–2 μm in size) can have beneficial effects on ceramic properties enhancing by two or three orders of magnitude its creep resistance. EXAFS analysis on yttria- and zirconia-doped alumina has indicated that dopants at the level of 100 ppm are mainly segregated to the alumina grain boundaries occupying probably substitutional Al sites. The mechanism by which the creep resistance is enhanced by doping has been postulated to be a reduction

* Corresponding author. Tel.: +33 4 72 43 62 39; fax: +33 4 72 43 85 28.
E-mail address: helen.reveron@insa-lyon.fr (H. Reveron).

0955-2219/$ – see front matter © 2007 Elsevier Ltd. All rights reserved.
doi:10.1016/j.jeurceramsoc.2007.04.015

of the grain-boundary diffusivity. In the case of yttria, segregation of Y to the alumina grain boundaries also modifies grain growth and intergranular fracture. Depending on the composition of Y (dilute, saturated, supersaturated and in equilibrium with YAG precipitates) the local environment around Y near the grain boundary is modified. The effect of these near-boundary layers on grain-boundary properties remains to be established.

The aim of this work is to reveal the effect of only silica on the sintering behaviour and microstructural evolution in alumina ceramics. We have studied the densification of an ultrapure α-alumina powder doped with small amounts of silica (500–2000 ppm), processed using colloidal approaches, slip-cast into alumina moulds and sintered under different atmospheres. The dopant segregation to the alumina grain boundaries was also characterized and correlated to the abnormal grain growth observed above a critical temperature of 1600 °C.

2. Experimental procedures

2.1. Raw materials

The ultrapure α-alumina AKP-50 (Sumitomo Chemical Company, Osaka, Japan) having an average particle size of 0.3 μm and an aqueous colloidal suspension containing only small silica particles of 22 nm (Ludox TMA, DuPont Co., Chemical and Pigments, Wilmington, DE) were used as starting materials.

We used the AKP-50 α-alumina because we were interested in studying the effect of only silica into its sintering behaviour and Sumitomo guarantee a purity of 99.99%. The chemical composition and characteristics of the as-received AKP-50 alumina powder are given in Table 1.

The silica was introduced using a colloidal suspension of very fine and monodisperse SiO_2 nanoparticles (22 nm) in order to enhance the dispersion of this material into the alumina matrix without modification of the pH of aqueous alumina suspensions. The use of such colloidal suspensions as doping source has been previously reported on alumina[11] and zirconia,[12] giving excellent results.

Table 1
Chemical composition and characteristics of the AKP-50 alumina powder

Composition	Characteristic	
	AKP-50 (values measured in this study)	AKP-50 (values provided from Sumitomo)
Si (ppm)	50 ± 10	<25
Ca (ppm)	30 ± 10	–
Na (ppm)	–	<10
Mg (ppm)	<15	<10
Cu (ppm)	–	<10
Fe (ppm)	–	<10
H_2O (%)	–	0.1
Particle size (μm)	0.35–0.4	0.1–0.3
Specific surface area (m^2/g)	14	9–15

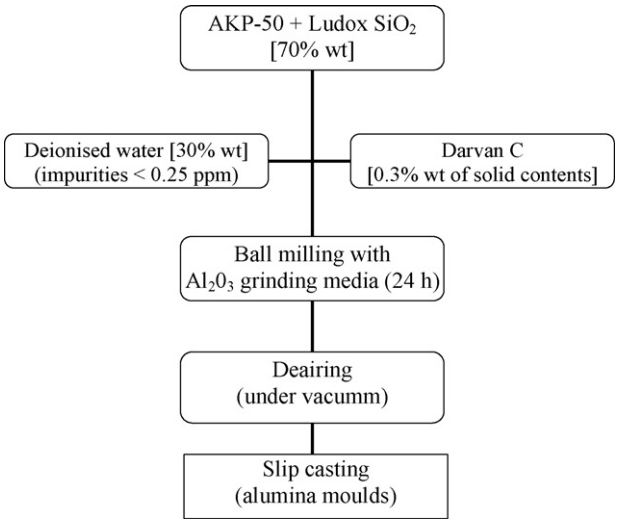

Fig. 1. Schematic diagram of the fabrication of green compacts of silica-doped alumina by the slip-casting technique.

2.2. Sample preparation and sintering

In this work, pure alumina and three different SiO_2–alumina-doped compositions were prepared (compositions by weight):

- A-0s: AKP-50 without doping.
- A-500s: AKP-50 + 500 ppm of SiO_2 (or 233 ppm of Si).
- A-1000s: AKP-50 + 1000 ppm of SiO_2 (or 466 ppm of Si).
- A-2000s: AKP-50 + 2000 ppm of SiO_2 (or 932 ppm of Si).

Green bodies were prepared by slip casting according to the procedure shown in Fig. 1. Porous alumina moulds were used in order to avoid any contamination. After drying, samples were sintered in a dilatometer (Setaram TMA 92 16/18) at different temperatures (1500–1700 °C for 2 h) and atmospheres (vacuum, static air and flowing air) using the same heating and cooling rate (300 °C/h).

2.3. Characterization

The pore volume was measured by mercury porosimetry (Micromeritics Autopore III 9420) and the bulk densities of sintered samples using Archimedes's method with deionised water as the immersion medium. Elemental analysis of powders and samples was performed by inductively coupled plasma-atomic emission spectrometry (ICP-AES) at the CNRS Central Service of Analysis, Vernaison-France. For microstructural examination, sintered samples were ground, polished to 1 μm finish and thermally etched to reveal the grain boundaries (at a temperature 50 °C lower than the sintering temperature, 20 min, 1500 °C/min). A scanning electron microscope (SEM Philips XL 30) was used to study polished surfaces which were coated with Au prior to observation. High-resolution transmission electron microscopy (HRTEM) and chemical analysis by energy-dispersive X-ray spectroscopy using nanoprobes (EDX) were performed on a Jeol 2010F instrument. Samples for HRTEM were prepared as follows: slices of 100 μm width were

(a)

Sample	Slurry pH
A-0s	9.4 - 9.6
A-500s	9.8 - 10.0
A-1000s	9.5 - 9.7
A-2000s	9.6 - 9.7

(b)

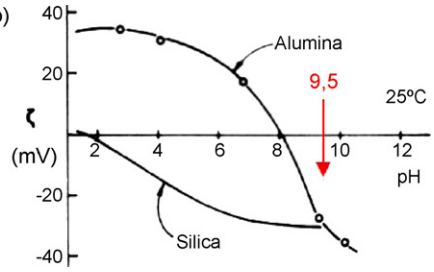

Fig. 2. (a) pH of aqueous slurries of AKP-50 alumina doping with 500, 1000 and 2000 ppm of silica and (b) zeta potential of the AKP-50 alumina and silica particles vs. pH.[6]

cut out of sintered samples using a diamond wire saw, then ground with a dimple-grinder to a thickness ranging between 30 and 10 μm and finally ion milled with argon ions at 4.5 keV. The phase analysis of powder and sintered samples was performed by X-ray diffractometry (Bruker HTXRD D8 Advance).

The sintering kinetics of pure AKP-50 alumina was investigated here using (a) nonisothermal and (b) isothermal experiments under static air at (a) 300, 600, 900 and 1200 °C/h up to 1300 °C and (b) 1070, 1090, 1110 and 1130 °C–6 h at 300 °C/h. The nonisothermal and isothermal techniques for analysis of the sintering allow for the determination of sintering parameters such as the sintering coefficient, activation energy and the n value. The n value can be related to the sintering mechanism (viscous flow, bulk diffusion or grain-boundary diffusion).[13]

3. Results and discussion

The use of an aqueous colloidal suspension as the source of SiO_2 allowed the preparation of different doped-alumina suspensions without modification of the natural basic pH obtained in the pure alumina slurry after the ball milling step (Fig. 2). The zeta potential versus pH data for the AKP-50 alumina and silica particles shows that for pH values above 9.5, alumina and silica surfaces are both charged negatively.[14] At the end of the ball milling step, highly stable and homogeneous doped slurries were obtained thanks to the resulting electrostatic repulsion forces. The hetero-coagulation approach developed to doping ceramics using colloidal suspensions[12] was not employed here because the attraction of the small quantities of silica by alumina would cause a heterogeneous repartition of the additive into the matrix.

The properties of green bodies obtained by slip casting are summarized in Table 2. Excepting the sample A-2000s, an excellent match between theoretical and measured Si contents was observed. For all compositions, the low measurement uncertainty can be related to a good and homogeneous dispersion of the colloidal silica into the alumina matrix taking into account that for each composition, some measurements were performed on different slip-cast samples obtained from the same slurry. The results show that green density is slightly increased by increasing the silica content.

Fig. 3 illustrates the effect of silica content on the densification of pure and doped-alumina sintered at 1500–1650 °C for 2 h and under static air. The introduction of silica slows down the densification process and leads to a significant reduction in density. This effect increases with the silica content and seems to start from the beginning of the sintering (first and/or intermediate stages) as already reported in the literature.[15–19] Nevertheless, only the density values of samples sintered above 1500 °C are displayed in Fig. 3 because the Archimedes's method cannot be used in materials sintered at lower temperatures. The dilatometric study revealed that the negative effect of silica on the densification is clearly observed from the end of the first sintering stage and during the intermediate stage ($T > 1200$ °C). We also observed that porosity started to decrease from 1200 to 1300 °C, corroborating the dilatometric results.

In the case of sintering pure AKP-50 alumina, using the nonisothermal method,[20,21] we calculated n values of 1.19 ± 0.03 between 1100 and 1200 °C (indicating a volume or bulk diffusion mass transport) and of 2.36 ± 0.12 between 1200 and 1270 °C (indicating a grain-boundary diffusion mechanism). Applying the isothermal method,[21] the n value of 1.56 ± 0.07 corroborated the bulk diffusion mechanism at $T < 1200$ °C.

Studying in detail the sintering behaviour of pure AKP-50 alumina we found that at 300 °C/h and between 1110 and 1200 °C (initial stage), sintering is controlled by a volumetric diffusion mechanism while between 1200 and 1270 °C (intermediate stage), sintering is controlled mainly by the diffusion in grain boundaries.[22] It seems to mean that the negative effect of

Table 2
Properties of slip-casted pure alumina and doped samples after drying (green bodies)

Sample	Theoretical Si composition (ppm)	Measured Si composition (ppm)[a]	Pore size[b] (μm)	Density ± 0.02 (g/cm^3)
A-0s	0	50 ± 10	0.0435	2.34
A-500s	233	245 ± 15	0.0374	2.38
A-1000s	466	480 ± 5	0.0381	2.36
A-2000s	932	810 ± 10	0.0509	2.37

[a] Some measures were performed on different samples elaborated by slip casting using the same slurry.
[b] Monomodal pore size distribution.

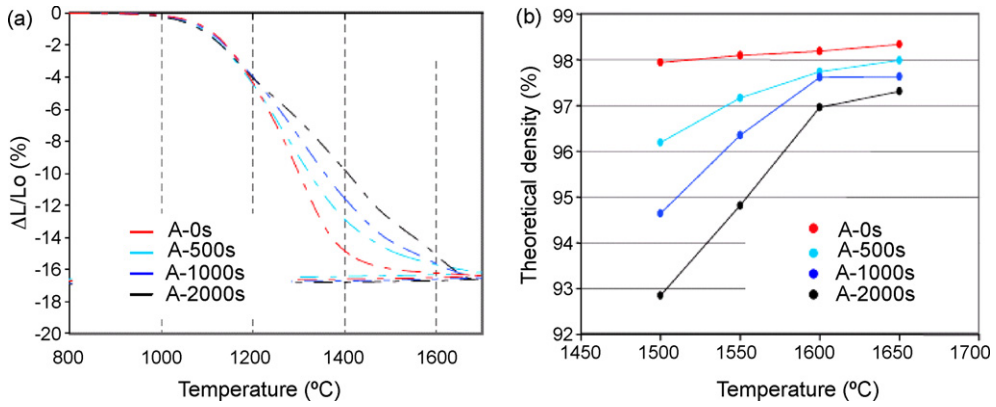

Fig. 3. Effect of silica content on the sintering behaviour of silica-doped alumina: (a) dilatometric study performed at a heating rate of 300 °C/h under static air for 2 h and (b) density of sintered samples.

silica starts when the sintering of alumina is controlled by the diffusion on grain boundaries mechanism.[23–25]

The evolution of the shrinkage rate versus the sintering temperature for SiO_2-doped samples is shown in Fig. 4. During the end of the first stage and at the intermediate stage of sintering (stage 2), an increase of silica content leads to an important decrease of the shrinkage rate (sintering anomaly which we called "B"). At higher temperatures (final stage of sintering or stage 3), a second sintering anomaly appears as a peak "P", which is more and more pronounced as the silica content increases.

To clarify the effect of silica on the densification behaviour, the localization of silicon atoms into the alumina lattice was studied. Below temperatures corresponding to the final stage of sintering ($T < T_{stage\,3}$), silicon was detected at grain-boundary triple junctions forming amorphous pockets as shown in Fig. 5a. HRTEM provided evidence of the amorphous nature of these pockets which appear disorganized in contrast with neighbouring well-crystallized grains (Fig. 5b) and EDX analysis confirmed the presence of silicon (1–2 at.%) and aluminium (Fig. 5c). As in the case of silica-doped 3Y-TZP ceramics materials quenched after sintering which exhibit silica-rich glassy phases both at grain boundaries and multiple junctions,[26] pockets could be formed from some silica particles which cannot diffuse into the alumina lattice, remaining consequently outside the grains. The aluminium (Al^{3+}) can arrive to these pockets trough a diffusion mechanism that will be much more important at high sintering temperatures.[27] Pockets located at the triple junctions are subjected to strong hydrostatic forces; therefore they are not able to crystallize due to thermodynamic equilibrium reasons.[28]

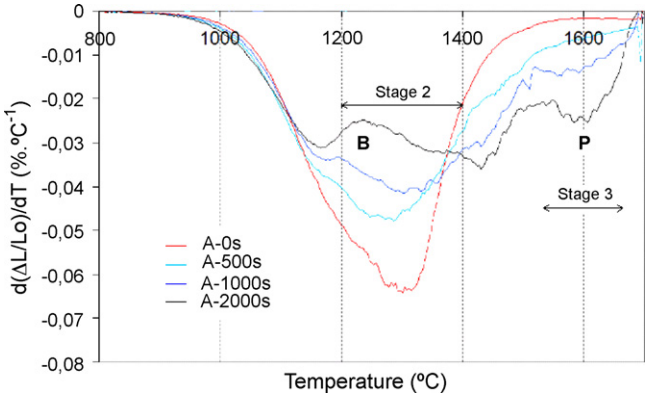

Fig. 4. Shrinkage rate vs. temperature for silica-doped aluminas (sintering under static air).

Fig. 6 shows a HRTEM micrograph and its corresponding EDX analysis performed on the sample A-2000s sintered at 1500 °C. For all the silica-doped samples sintered below 1500 °C, no glassy and/or secondary phases were detected at any grain boundary (gb). EDX line scans showed a systematic dopant enrichment at the vicinity of the grain boundaries and not inside the grains (grain silicon content < limit of EDX detection) as shown in Fig. 6. The silicon was detected over at least 10 nm to each side of the grain boundary in A-2000s sintered sample. Segregation of cations (Ca, Ti, Mn and Si) at the vicinity of the alumina grain boundaries has been observed before.[29–39] Authors who have reported such a segregation phenomenon always insisted on the approximate values which can be extracted from EDX quantitative analysis performed on small distances. However, from a qualitative point of view, this phenomenon has been already shown. In our study, the dopant enrichment detected over a probe's movement distance >10 nm (A-2000s), does not appear attributable to spatial resolution problems. The difference in silicon content between grains and the crystalline zones neighbouring the grain boundaries may be explained in terms of the formation of a solid solution at the grain boundary as shown firstly by Harmer et al.[1,40–44]

We observed that the sintering anomaly "B" becomes more pronounced by increasing the quantity of dopant (Fig. 4). In the literature, the proposed interpretations to explain such a phenomenon remain very controversial: multimodal porosity sizes,[45–47] alumina phase transformations,[48,49] the Kirkendall's effect,[50] the crystallization of new compounds,[27,51] the formation of intergranular liquid phases[27,52] or the modification of point defect concentrations[53–56] have been proposed. In the present study only the latest hypothesis seems to be responsible for the sintering anomaly "B" because (a) pore size distribution was always monomodal during sintering (no multimodal porosity effect was observed by Hg porosimetry as shown in Fig. 7), (b) only the α-alumina phase was presented in the alu-

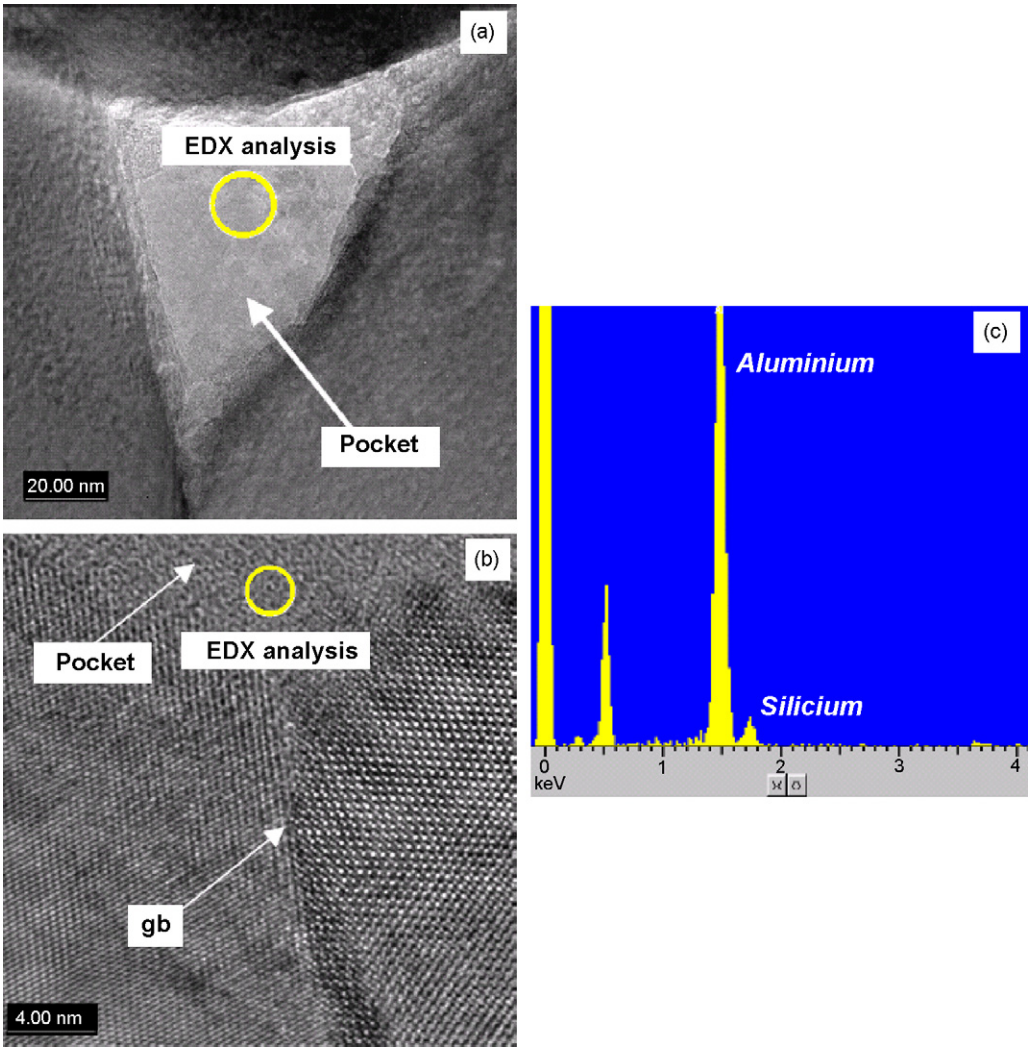

Fig. 5. Amorphous pockets at the grain-boundary triple junctions formed in silica-doped sample (A-2000s) sintered 2 h at 1500 °C under static air (below the sintering anomaly "P"): (a) TEM micrograph, (b) HRTEM micrograph and (c) EDX analysis.

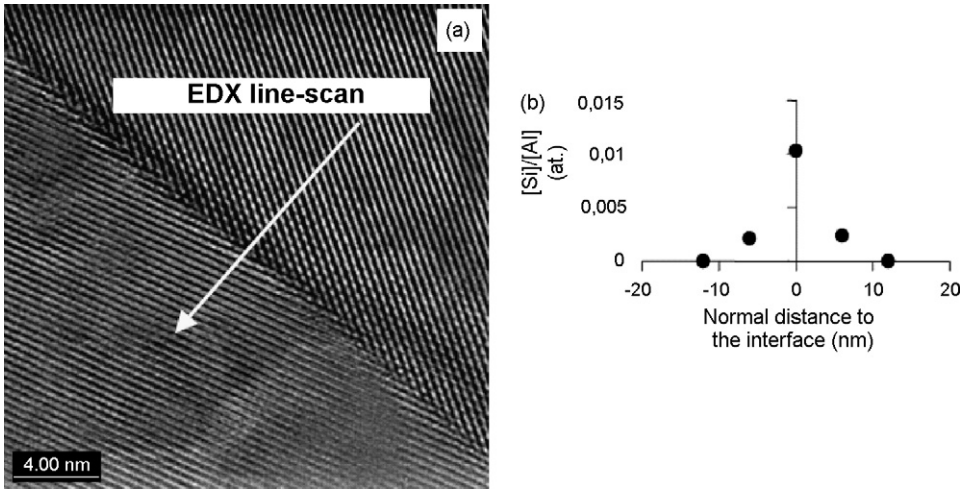

Fig. 6. Grain boundary in silica-doped sample (A-2000s) sintered 2 h at 1500 °C under static air (below the sintering anomaly "P"): (a) HRTEM micrograph and (b) EDX line-scan.

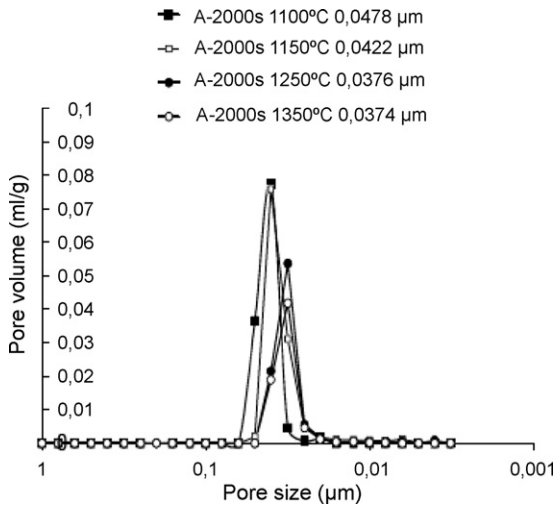

Fig. 7. Pore size distribution in silica-doped sample (A-2000s) sintered at different temperatures.

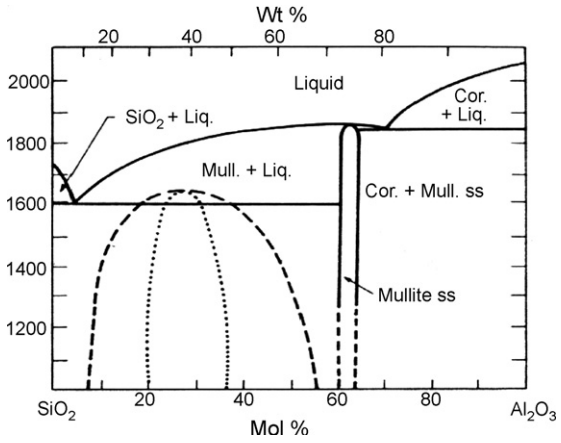

Fig. 9. Al_2O_3–SiO_2 binary phase diagram.

mina AKP-50, (c) Kirkendall's pores never were observed in sintered doped-aluminas as will be discussed later and finally (d) the HRTEM investigations performed on 1500 °C sintered samples did not show the presence of intergranular amorphous phases at ambient temperature. The preferential dissolution of silicon at the grain boundaries of alumina (Fig. 6) may effectively modify the concentration of the point defects in these interfaces.[53,54] Introducing silicon atoms into alumina lattice ($3SiO_2 = 3SiO_{Al^o} + V''_{Al} + 6O^x_o$ or $2SiO_2 = 2Si_{Al^o} + O''_i + 3O^x_o$) results in an increase of aluminium vacancies (V''_{Al}) or interstitial oxygen (O''_i) and in a subsequently decrease of interstitial aluminium atoms (Al_i^{ooo}) and/or oxygen vacancies ($V_O{}^o$). Because point defects are known to favour diffusion processes, the slow down on sintering rate of silica-doped samples can be related to a falling in Al_i^{ooo} and/or $V_O{}^{oo}$ concentration. Some sintering experiments performed under different atmospheres provided evidence. It is well known that atmosphere plays two

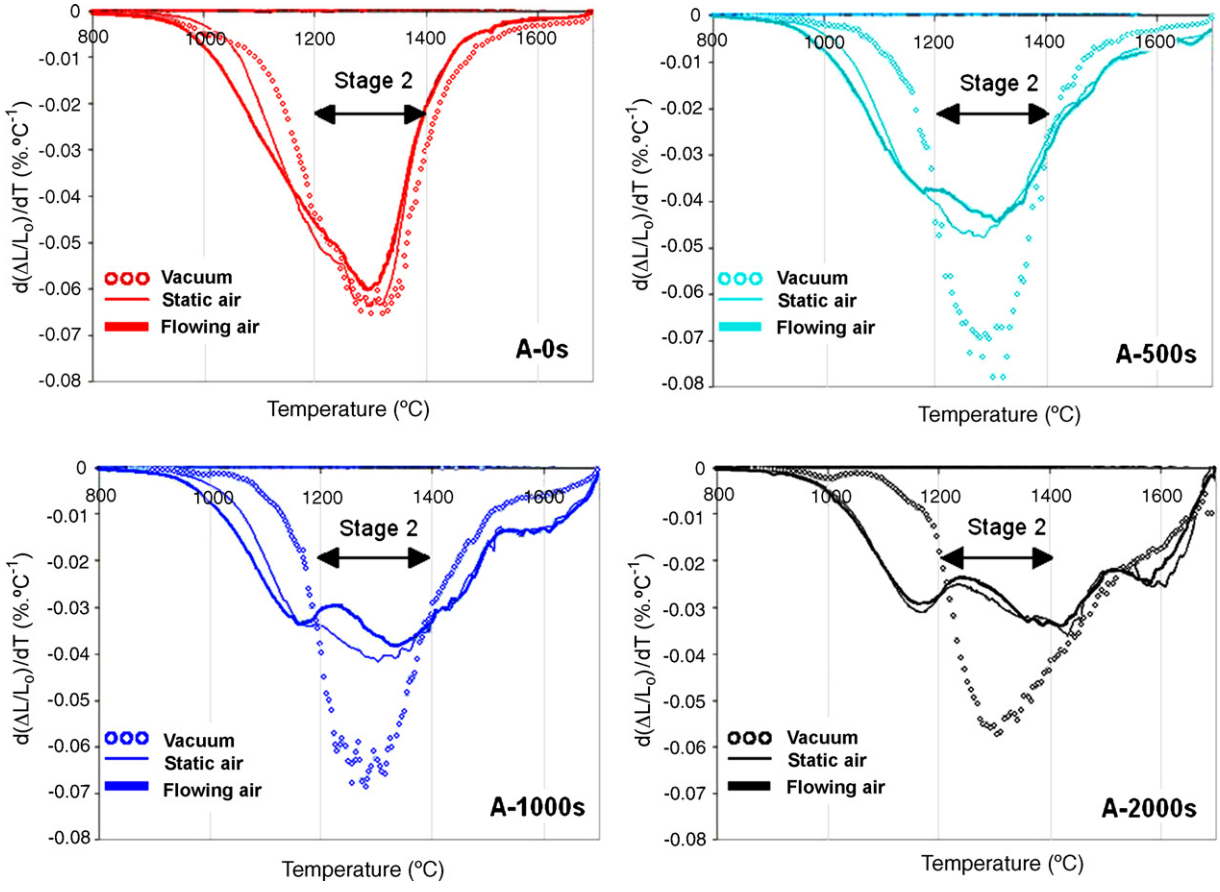

Fig. 8. Shrinkage rate vs. temperature for silica-doped aluminas sintered under different atmospheres.

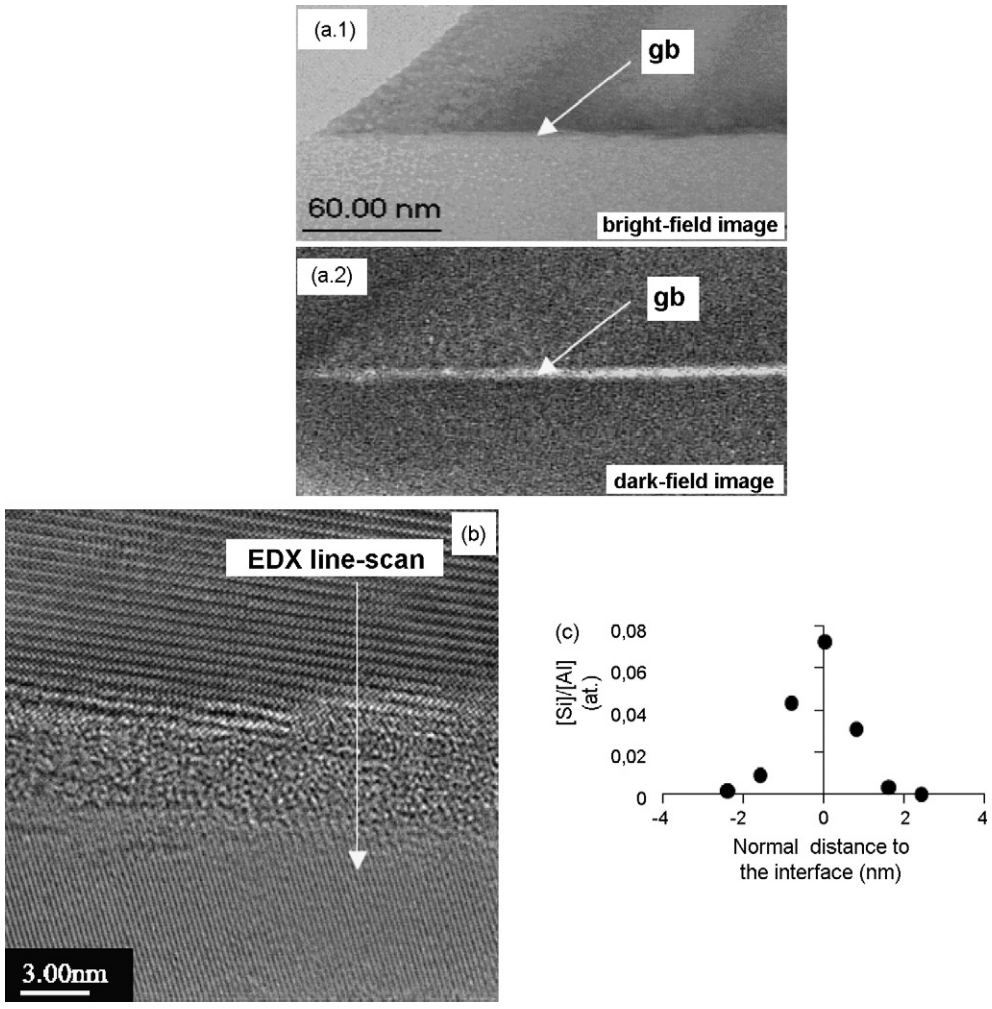

Fig. 10. Aluminosilicate glassy films at the grain boundary in silica-doped sample (A-2000s) sintered 2 h at 1650 °C under static air (above the sintering anomaly "P"): (a) bright and dark field TEM micrographs, (b) HRTEM micrograph and (c) EDX line-scan.

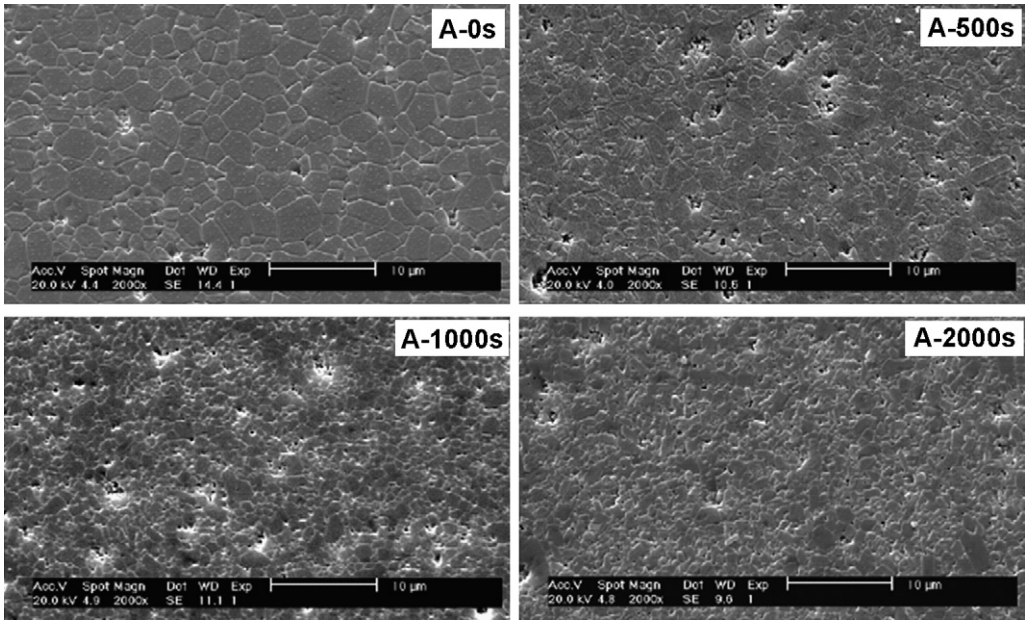

Fig. 11. SEM micrographs of pure and doped-alumina samples sintering at 1550 °C (below "P") for 2 h and under static air: (a) A-0s, (b) A-500s, (c) A-1000s and (d) A-2000s.

principal roles during sintering: along the whole of this process it modifies the point defect concentrations[57] and at the last stage of sintering it can be trapped inside the closed porosity.[58,59] Low oxygen partial pressures (e.g. sintering under vacuum) will be unfavourable to silicon incorporation into α-alumina, since it promotes point defects such as oxygen vacancies (V_O^{oo}) and aluminium interstitials (Al_i^{ooo}),[33,60] whereas sintering under oxidizing atmospheres (e.g. sintering under flowing air) will lead to the opposite behaviour. Fig. 8 shows the effect of three different atmospheres (vacuum, static air and flowing air) on the sintering shrinkage rate of pure and silica-doped samples. It is interesting to note that the atmosphere effect is always the same, independent of the sample composition. Taking as a reference the less oxidizing atmosphere (vacuum), we observe that the slow down in densification rate becomes much more important by enhancing the oxygen content (static and flowing air, respec-

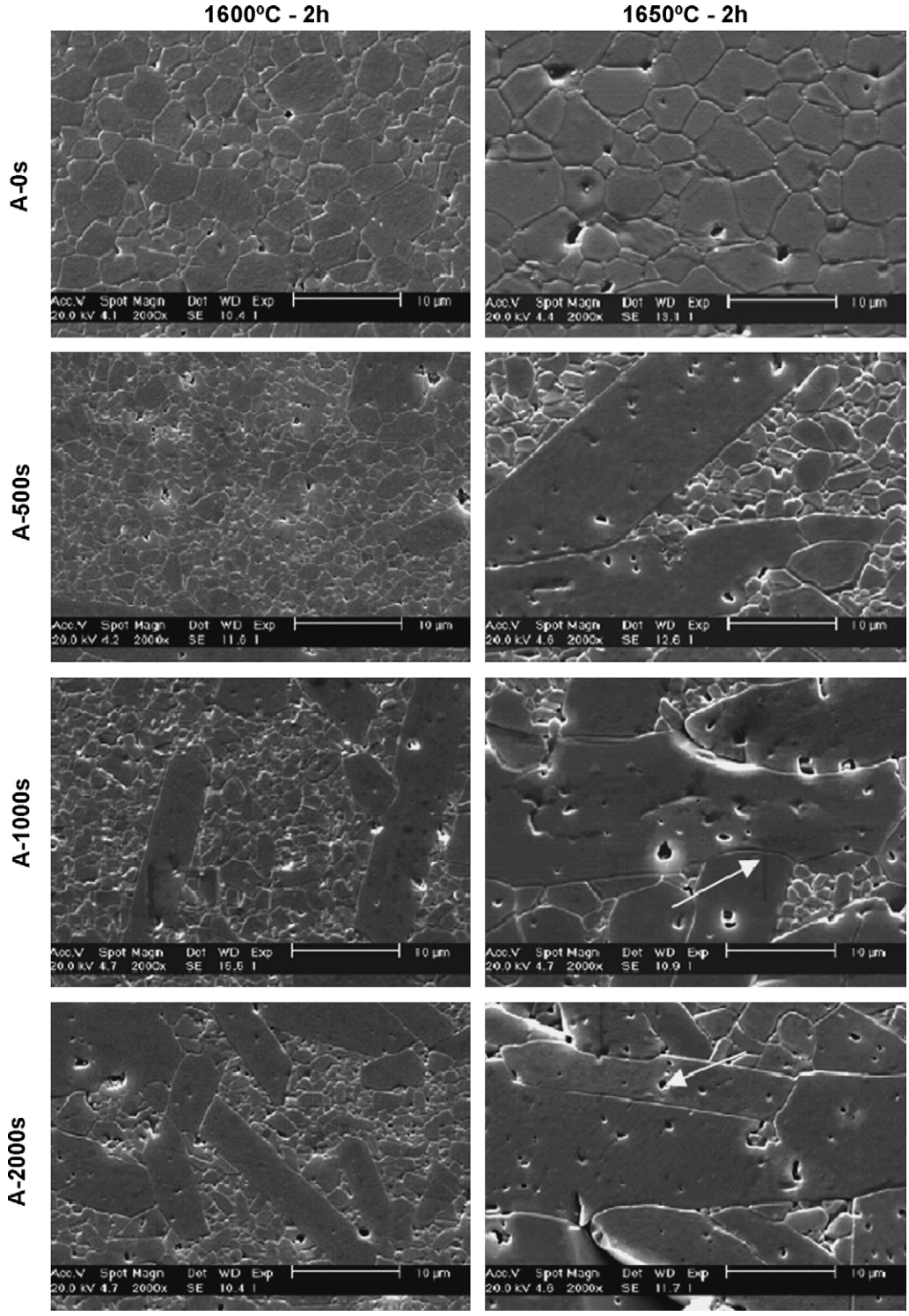

Fig. 12. SEM micrographs of pure and doped-alumina samples sintering at 1600 and 1650 °C (above "P") for 2 h and under static air.

tively). Moreover, the sintering anomaly "B" was not observed in doped-samples sintered under vacuum. Oxidizing atmospheres has qualitatively the same effect as an increase in silica content because the incorporation of silicon into alumina lattice leads to oxygen vacancies and/or aluminium interstitials point defects. Some thermoluminescence experiments performed on doped samples showed us that oxygen vacancies was predominantly removed after doping or under oxidizing conditions (these results will be published soon). The silicon segregation at the grain boundaries (forming solid solution) would slow down the diffusion mechanisms due to a predominant decrease of oxygen point defects from 1200 °C. As pointed out previously, the alumina densification is controlled by a mechanism of diffusion at the grain boundaries above 1200 °C. The detrimental effect of silica on the alumina densification during the stage 2 of sintering (1200–1400 °C) can be explained by this fact.

The second sintering anomaly "P", which is more and more pronounced as the silica content increases, appears during the final stage of sintering (stage 3 in Fig. 4: 550–1650 °C). The peak "P" is located at a temperature of $T_{\text{anomaly P}} \sim 1580$ °C which is very close to the lower eutectic temperature in the system Al_2O_3–SiO_2 (Fig. 9). Microstructural characterization of doped-alumina sintered at 1650 °C revealed considerable differences (Fig. 10). An amorphous phase clearly appears at some grain boundaries as observed by TEM. The thickness of these intergranular amorphous films was 2–3 nm in A-2000s samples. The line-scan EDX analysis showed a silicon enrichment of these films compared to the bulk and the presence of aluminium. Nevertheless, the silicon enrichment is much less spread to each side of the grain boundary (only 2 nm) than in samples sintered at 1500 °C (stage 2), in which silicon segregation reached at least 10 nm. In samples sintered at temperatures above the anomaly "P", silicon is only presented into this 2–3 nm aluminosilicate glassy phase. Similar results have been reported in the literature for pure silicon amorphous films (2 nm) or aluminosilicate films (3.7 nm) at the grain boundaries. However, the reports on aluminosilicate glassy phases in alumina exclusively doped with silica are rare.[40] The anomaly "P" shown in Fig. 4 can be related to the formation of an intergranular liquid phase which enhances densification in doped-samples (increase on shrinkage rates).[16,59,61–63] This liquid phase is transformed into a glassy phase when samples are cooled down, as observed in Fig. 10. The existence of a link between the silicon solid solution formed at the grain boundaries (1200–1400 °C) and the glassy phase observed at these interfaces after sintering at temperatures close to the lower Al_2O_3–SiO_2 eutectic, allows us to propose a transitional liquid phase formation.[1] As the silicon is introduced preferentially at the grain boundaries (solid solution), only some regions saturated in silica can reach the SiO_2-rich eutectic composition (Fig. 9). This can explain why we do not observe the glassy phase at all doped-silica alumina grain boundaries.

The microstructures of alumina and doped-aluminas sintered at a temperature below the anomaly "P" and under static air are shown in Fig. 11. The grain size seems to become smaller with the increase in silica. A similar effect of silica over the grain size of α-alumina has been already observed.[15,18,44] This behaviour could be attributed to the slow down of grain migration rate due to the formation of solid solutions at the grain boundaries. Whatever the composition of the sample, no abnormal grain growth was observed after sintering at 1550 °C for 2 h.

Above the sintering anomaly "P", strong microstructural changes were observed. SEM investigations in pure and silica-doped samples confirm the well-known correlation between liquid phases at the grain boundaries and heterogeneous microstructures. As shown in Fig. 11, abnormal grain growth occurred at the temperatures above 1600 °C in only silica-doped aluminas. This abnormal grain growth is enhanced by doping: the microstructure of the sample doped with 2000 ppm of silica (A-2000s) and sintered at 1650 °C consisted of only plate-like large grains. During the grain growing process grains can block themselves, curbing the abnormal growth process. Some lengthened grains seem to penetrate other grains as shown by an arrow on the micrograph of the sample A-1000s sintered at 1650 °C (Fig. 12). It is interesting to note that in doped samples, the pores are mainly located at intragranular positions (white arrow on the micrograph of the sample A-2000s sintered at 1650 °C). At high temperatures, the formation of an intergranular liquid phase promotes abnormal grain growth and intragranular porosity (the rate of pore migration being lower than the rate of boundaries migration).

4. Conclusions

The addition of small quantities of colloidal silica to a commercial α-alumina powder has a significant effect on its densification and microstructure evolution.

Silica has a detrimental effect on the alumina densification behaviour particularly during the intermediate stage of sintering (from 1200 to 1400 °C). We showed that in this temperature range, the silicon forms a localized solid solution at the alumina grain boundaries most probably resulting in a decrease of the oxygen vacancies concentration. Such defect decrease affects the diffusion processes during sintering producing a strong slow down of the shrinkage rate.

At higher temperatures, silica allowed the formation of an intergranular liquid phase which leads to abnormal grain growth in the final stage of sintering (1550–1650 °C). An increase of sintering shrinkage rates was observed (anomaly called by us "P") follows the formation of the liquid phase. Nevertheless, densification to the theoretical density was then prevented because some pores remain trapped within or between the abnormally grown large grains.

Acknowledgement

The authors wish to thank Thierry Epicier (CECM/Insa-Lyon) for TEM/HRTEM microstructural characterizations.

References

1. Bae, S. I. and Baik, S., Determination of critical concentration of silica and/or calcia for abnormal grain growth in alumina. *J. Am. Ceram. Soc.*, 1993, **76**(4), 1065–1067.

2. Park, C. W. and Yoon, D. Y., Effects of SiO_2, CaO_2, and MgO additions on the grain growth of alumina. *J. Am. Ceram. Soc.*, 2000, **83**(10), 2605–2609.
3. Gavrilov, K. L., Bennison, S. J., Mineska, K. R., Chabala, J. M. and Levi-Setti, R., Silica and magnesia dopant distributions in alumina by high-resolution scanning secondary ion mass spectrometry. *J. Am. Ceram. Soc.*, 1999, **82**(4), 1001–1008.
4. Jung, J. and Baik, S., Abnormal grain growth of alumina: CaO effect. *J. Am. Ceram. Soc.*, 2003, **86**(4), 644–649.
5. McLaren, I., Cannon, R. M., Gülgün, M. A., Voytovych, R., Popescu-Pogrion, N., Scheu, C., Taffner, U. and Rühle, M., Abnormal grain growth in alumina: synergistic effects of yttria and silica. *J. Am. Ceram. Soc.*, 2003, **86**(4), 650–659.
6. Altay, A. and Gülgün, M. A., Microstructural evolution of calcium-doped α-alumina. *J. Am. Ceram. Soc.*, 2003, **86**(4), 623–629.
7. French, J., Zhao, J., Harmer, M. P., Chan, H. M. and Miller, G. A., Creep of duplex microstructures. *J. Am. Ceram. Soc.*, 1994, **77**(11), 2857–2865.
8. Wang, C. M., Cargill, G. S., Harmer, M. P., Chan, H. M. and Cho, J., Atomic structural environment of grain boundary segregated Y and Zr in creep resistant alumina from EXAFS. *Acta Mater.*, 1999, **47**(12), 3411–3422.
9. Cho, J., Wang, C. M., Chan, H. M., Rickman, J. M. and Harmer, M. P., Role of segregating dopants on the improved creep resistance of aluminium oxide. *Acta Mater.*, 1999, **47**(15), 4197–4207.
10. Wang, C. M., Cargill, G. S., Chan, H. M. and Harmer, M. P., Structural features of Y-saturated and supersaturated grain boundaries in alumina. *Acta Mater.*, 2000, **48**, 2579–2591.
11. Kebbede, A., Parai, J. and Carim, A. H., Anisotropic grain growth in α-Al_2O_3 with SiO_2 and TiO_2 additions. *J. Am. Ceram. Soc.*, 2000, **83**(11), 2845–2851.
12. Gremillard, L., Chevalier, J., Epicier, T. and Fantozzi, G., Improving the durability of biomedical-grade zirconia ceramic by the addition of silica. *J. Am. Ceram. Soc.*, 2002, **85**(2), 401–407.
13. Woolfrey, J. L. and Bannister, M. J., Nonisothermal techniques for studying initial-stage sintering. *J. Am. Ceram. Soc.*, 1972, **55**(8), 390–394.
14. Agrawal, D. C., Raj, R. and Cohen, C., In-situ measurements of silica-gel coating on particles of alumina. *J. Am. Ceram. Soc.*, 1990, **73**(7), 2163–2164.
15. Lee, K. Y., Lee, Y. H., Kim, H. I., Han, K. W. and Park, J. M., The influence of sintering additives on the lifetime of the heater for sensor application with Al_2O_3 substrate. *Mater. Lett.*, 1998, **37**, 90–97.
16. Goswami, A. P., Roy, S., Mitra, K. and Das, J. C., Impurity-dependent morphology and grain growth in liquid-phase-sintered alumina. *J. Am. Ceram. Soc.*, 2001, **84**(7), 1620–1626.
17. Louet, N., Gonon, M. and Fantozzi, G., Influence of the amount of Na_2O and SiO_2 on the sintering behavior and on the microstructural evolution of a Bayer alumina powder. *Ceram. Int.*, 2005, **31**, 981–987.
18. Sumita, S. and Bowen, H. K., Effects of foreign oxides on grain growth and densification of sintered Al_2O_3. In *Ceramic Transactions, Vol. 21: Ceramics Powder Science II*, ed. P. A. Pask and A. G. Evans. Plenum Publishers, New York, 1988, pp. 840–847.

[19]. Louet, N., Epicier, T. and Fantozzi, G., Investigation of the sintering behaviour of ultrapure α-alumina containing low amounts of SiO_2 and CaO. In *The Science of Engineering of Ceramics III*, ed. T. Ohji, T. Sekino and K. Niihara. Trans. Tech. Pub., Switzerland, 2006, pp. 61–66.

20. Wang, J. and Raj, R., Estimate the activation energies for boundary diffusion from rate controlled sintering of pure alumina, and alumina doped with zirconia and titania. *J. Am. Ceram. Soc.*, 1990, **73**(5), 1172–1175.
21. Johnson, D. L. and Cuttler, I. B., Diffusion sintering. II. Initial sintering kinetics of alumina. *J. Am. Ceram. Soc.*, 1970, **46**(11), 545–550.
22. Bannister, M. J., Shape sensitivity of initial sintering equations. *J. Am. Ceram. Soc.*, 1968, **51**(10), 548–553.
23. Johnson, D. L. and Cuttler, J. B., Diffusion sintering. II. Initial sintering kinetics of alumina. *J. Am. Ceram. Soc.*, 1963, **46**(11), 545–550.
24. Bagley, R. D. and Lynn Johnson, D., Effect of TiO_2 on initial sintering of Al_2O_3. *J. Am. Ceram. Soc.*, 1970, **5**(3), 136–141.
25. Messing, G. L. and Kumagal, M., Low-temperature sintering of α-alumina-seeded boehmite gels. *Am. Ceram. Soc. Bull.*, 1994, **73**, 88–91.
26. Gremillard, L., Epicier, T., Chevalier, J. and Fantozzi, G., Effect of cooling rate on the location and chemistry of glassy phases in silica-doped 3Y-TZP ceramics. *J. Eur. Ceram. Soc.*, 2005, **25**(6), 875–882.
27. Michalet, T., Palier, M., Berclin, F., Duclos, R. and Crampon, J., Elaboration of low shrinkage mullite by active filler controlled pyrolysis of siloxanes. *J. Eur. Ceram. Soc.*, 2002, **22**, 143–152.
28. Raj, R. and Lange, F. F., Crystallization of small quantities of glass (or liquid) segregated in grain boundaries. *Acta Metall.*, 1981, **29**, 1993–2000.
29. Monceau, D., Petot, C., Petot-Ervas, G., Fraser, J. W., Fraser, M. J., Graham, M. J. and Sproule, G. L., Surface segregation and morphology of Mg-doped α-alumina powders. *J. Eur. Ceram. Soc.*, 1995, **15**, 851–858.
30. Wakai, F., Nagano, T. and Iga, T., Hardening in creep of alumina by zirconium segregation at the grain boundary. *J. Am. Ceram. Soc.*, 1997, **80**(9), 2361–2366.
31. Baik, S. and White, C. L., Anisotropic calcium segregation to the surface of Al_2O_3. *J. Am. Ceram. Soc.*, 1987, **70**(9), 682–688.
32. Bagley, R. D. and Lynn Johnson, D., Effect of magnesia on grain growth in alumina. *Adv. Ceram.*, 1984, **10**, 666–678.
33. Loudjani, M. K. and Haut, C., Influence of the oxygen pressure on the chemical state of yttrium in polycrystalline α-alumina. Relation with microstructure and mechanical toughness. *J. Eur. Ceram. Soc.*, 1996, **16**, 1099–1106.
34. Kebbede, A. H. and Carim, A. H., Segregation of Si and Ti in α-alumina. *Mater. Lett.*, 1999, **41**, 198–203.
35. Wang, C. M., Cargill III, G. S., Harmer, M. P., Chan, H. M. and Cho, J., Atomic structural environment of grain boundary segregated Y and Zr in creep resistant alumina from EXAFS. *Acta. Mater.*, 1999, **47**, 3411–3422.
36. Morgan, P. E. D. and Koutsoutis, M. S., Phase studies concerning sintering in aluminas doped with Ti^{4+}. *J. Am. Ceram. Soc.*, 1985, **68**(6), C156–C158.
37. Taylor, R. I., Coad, J. P. and Brook, R. J., Grain boundary segregation in Al_2O_3. *J. Am. Ceram. Soc.*, 1974, **57**(12), 539–540.
38. Cook, R. F. and Schrott, A. G., Calcium segregation to grain boundaries in alumina. *J. Am. Ceram. Soc.*, 1988, **71**(1), 50–58.
39. Baik, S. and Moon, J. H., Effects of magnesium oxide on grain-boundary segregation of calcium during sintering of alumina. *J. Am. Ceram. Soc.*, 1991, **74**(4), 819–822.
40. Lee, C. H. and Kröger, F. A., Electrical conductivity of polycrystalline Al_2O_3 doped with silicon. *J. Am. Ceram. Soc.*, 1985, **68**(2), 92–99.
41. Litton, D. A. and Garofalini, S. H., Atomistic structure of sodium intergranular films in alumina. *J. Mater. Res.*, 1999, **14**, 1418–1429.
42. Susnitsky, D. W. and Carter, C. B., Structure of alumina grain boundaries prepared with and without a thin amorphous intergranular film. *J. Am. Ceram. Soc.*, 1990, **73**(8), 2485–2493.
43. Yoshida, H., Ikuhara, Y. and Sakuma, T., Grain boundary electronic structure related to the high-temperature creep resistance in polycrystalline Al_2O_3. *Acta Mater.*, 2002, **50**, 2955–2966.
44. Kim, Y. M., Hong, D. and Kim, Y., Anisotropic abnormal grain growth in TiO_2/SiO_2-doped alumina. *J. Am. Ceram. Soc.*, 2000, **83**(11), 2809–2812.
45. Kimura, T., Matsuda, Y., Oda, Y. and Yamaguchi, T., Effects of agglomerates on the sintering of alpha-Al_2O_3. *Ceram. Int.*, 1987, **13**, 27–34.
46. Dynys, F. W. and Halloran, J. X., Influence of aggregates on sintering. *J. Am. Ceram. Soc.*, 1984, **67**(9), 596–601.
47. Shi, J. L. and Yen, T. S., Densification and microstructure development of alumina/Y-TZP composite powder (Y-TZP-rich). *J. Eur. Ceram. Soc.*, 1995, **15**, 363–369.
48. Bloche, B., Ravi, B. G. and Chaim, R., Stabilization of transition alumina and grain growth inhibition in ultrafine Al_2O_3–5 wt.% SrO alloy. *Mater. Lett.*, 2000, **42**, 61–65.
49. He, Z. and Ma, J., Densification and grain growth during interface reaction controlled sintering of alumina ceramics. *Ceram. Int.*, 2001, **27**, 261–264.
50. Kolar, D. and Stadler, Z., Sintering in multicomponent systems. In *Proceeding of International Symposium of Factors on Densification and Sintering of Oxide and Non-oxides Ceramics*, ed. S. Somiya and S. Saito, 1978, pp. 206–227.
51. Pask, J. K., Zhang, X. W. and Tomsia, A. P., Effect of sol–gel mixing on mullite microstructure and phase equilibria in the α-Al_2O_3–SiO_2 system. *J. Am. Ceram. Soc.*, 1987, **70**(10), 704–707.
52. Aksay, L. A. and Pask, J. A., Stable and metastable equilibria in the system SiO_2–Al_2O_3. *J. Am. Ceram. Soc.*, 1975, **58**(11/12), 507–512.
53. Monty, C. and Atkinson, A., Grain-boundary mass transport in ceramic oxides. *Cryst. Latt. Def. Amorph. Mater.*, 1989, **18**, 97–120.

54. Prot, D., Le Gall, M., Lesage, B., Huntz, M. and Monty, C., Self-diffusion in α-Al_2O_3. IV. Oxygen grain-boundary self-diffusion in undoped and yttria-doped alumina polycrystals. *Phil. Mag. A*, 1996, **73**, 935–949.
55. Kutty, T. R. G., Hedge, P. V., Khan, K. B., Majumdar, S. and Purushotham, D. S. C., Sintering studies on UO_2–PuO_2 pellets with varying PuO_2 content using dilatometry. *J. Nucl. Mater.*, 2000, **282**, 54–65.
56. Kutty, T. R. G., Khan, K. B., Hedge, P. V., Sengupta, A. K., Majundar, S. and Purushotham, D. S. C., Densification behaviour and sintering kinetics of PuO_2 pellets. *J. Nucl. Mater.*, 2001, **297**, 120–128.
57. Pae, Y. K., Eun, K. Y. and Kang, S. J. L., Effect of Sintering atmosphere on densification of MgO-doped Al_2O_3. *J. Am. Ceram. Soc.*, 1988, **71**(8), C380–C382.
58. Coble, R. L., Sintering alumina: effect of atmospheres. *J. Am. Ceram. Soc.*, 1962, **45**(3), 123–127.
59. Yan, M. F., Effects of physical, chemical, and kinetic factors on ceramic sintering. In *Advanced Ceramics 21: Ceramic Powder Science*. American Ceramic Society, 1987, pp. 635–669.
60. Gavriliu, G. and Tardei, C., Influence of the sintering atmosphere on the compacting of high alumina ceramics. In *Ceramics Today: Tomorrow's Ceramics*. Elsevier Science Publishers B.V., 1991, pp. 1425–1431.
61. Kostic, E., Boskovic, S. and Kiss, S. J., Reaction sintering of Al_2O_3 in the presence of the liquid phase. *Ceram. Int.*, 1993, **19**, 235–240.
62. Boskovic, S., Kostic, E. and Cerovic, D., Sintering of inactive alumina in the presence of oxide and nonoxide additions. *Adv. Ceram.*, 1988, **20**, 26–31.
63. Suvaci, E., Oh, K. S. and Messing, G. L., Kinetics of template growth in alumina during the process of templated grain growth (TGG). *Acta Mater.*, 2001, **49**, 2075–2081.